power density can be reduced by a factor of four as compared to a single horn feed. Additional reduction is possible by proper selection of feed defocusing.

REFERENCES

[1] L. J. Ricardi and L. Niro, "Design of a twelve-horn monopulse feed," in *1961 IRE Int. Convention Rec.*, part 1, pp. 93–102.
[2] P. W. Hannan, "Optimum feed for all three modes of a monopulse antenna II: Practice," *IRE Trans. Antennas Propagat.*, vol. AP-9, pp. 454–461, Sept. 1961.
[3] N. Amitay and H. Zucker, "Compensation of spherical reflector aberrations by planar array feeds," *IEEE Trans. Antennas Propagat.*, vol. AP-20, pp. 49–56, Jan. 1972.
[4] A. R. Dion and L. J. Ricardi, "A variable coverage satellite antenna system," *Proc. IEEE*, vol. 59, pp. 252–262, Feb. 1971.
[5] S. Silver, *Microwave Antenna Theory and Design* (Radiation Lab. Series, vol. 12). New York: McGraw-Hill, 1949, p. 4.

On Thin-Wire Multiturn Loop Antennas

CLAYBORNE D. TAYLOR, MEMBER, IEEE, AND CHARLES W. HARRISON, JR., FELLOW, IEEE

Abstract—**A general theory of thin-wire multiturn loop antennas is presented. For convenience the windings of the loop are considered to form a circular helix. An integral equation is derived and solved numerically for the current distribution on the antenna. The antenna impedance, efficiency, and pattern are obtained.**

INTRODUCTION

THE MULTITURN loop antenna has important applications as both a transmitting and a receiving antenna, primarily because the volume occupied by the antenna is not required to have dimensions comparable to the operating wavelength. However, the multiturn loop is formidable to analyze because of its somewhat complex physical configuration. In particular it is difficult to determine the high frequency behavior. In this paper a multiturn loop in the form of a circular helix is considered, and a general theoretical–numerical formulation is presented.

The single-turn loop antenna has been studied by a number of investigators [1]–[6]. Generally a delta function generator is used for the driving mechanism in the analysis; however, in the formulation presented here a magnetic ring source is used. Recently the polygon loop antenna, single turn and multiturn, was studied by using the so-called reaction technique developed by Richmond [7], [8].

By using certain symmetry properties and judicious approximations, Padhi [9] has developed a theory of multiturn loop antennas with particular winding configurations. Recently, Smith [10] developed a formulation for electrically small multiturn loops. Also, Smith considered proximity effects on the circumferential current distribution about the wire element cross section. The research reported here is not restricted to electrically small loops and is more general than that presented by Padhi.

Manuscript received October 24, 1972; revised January 7, 1974. This work was supported in part by the Ballistics Research Laboratories, Aberdeen Proving Ground, Md., and the U. S. Atomic Energy Commission.

C. D. Taylor is with the Department of Electrical Engineering, Mississippi State University, State College, Miss. 39762.
C. W. Harrison, Jr., was with Sandia Laboratories, Albuquerque, N. Mex. He is now with General Electro-Magnetics, Albuquerque, N. Mex.

ANALYSIS

Consider the multiturn loop antenna to be in the form of a circular helix with the following parametric equations:

$$x = R_0 \cos\theta$$
$$y = R_0 \sin\theta$$
$$z = p\theta/2\pi \tag{1}$$

where θ is the parameter, R_0 is the radius of the helix, and p is the pitch of the helix. The parameter θ may be expressed in terms of arc length along the helix; i.e.,

$$\theta = \alpha s \tag{2}$$

where

$$\alpha = [R_0^2 + (p/2\pi)^2]^{-1/2}. \tag{3}$$

The vector and scalar potentials, when evaluated on the axis of the wire forming the multiturn loop, may be written [11]

$$A_s(s) = \frac{\mu}{4\pi}\int_L ds'\ (\hat{s}\cdot\hat{s}')I_s(s')G(s,s') \tag{4}$$

$$\phi(s) = -j\frac{\eta}{4\pi k}\int_L ds'\frac{d}{ds'}[I_s(s')]G(s,s') \tag{5}$$

where

$$G(s,s') = \exp[-jk(R^2(s,s') + a^2)^{1/2}]/(R^2(s,s') + a^2)^{1/2} \tag{6}$$

$$R^2(s,s') = (2R_0)^2\sin^2[\alpha(s - s')/2] + (\alpha p/2\pi)^2(s - s')^2 \tag{7}$$

$$\hat{s}\cdot\hat{s}' = (\alpha R_0)^2\cos[\alpha(s - s')] + (\alpha p/2\pi)^2. \tag{8}$$

In these expressions a is the radius of the wire forming

the multiturn loop and $\eta = (\mu/\epsilon)^{1/2}$ is the intrinsic wave impedance of the surrounding medium.

On the axis of the wire the component of the total electric field tangent to the axis is

$$E_s(s) = E_s^{\text{inc}}(s) - \frac{d}{ds}\phi(s) - j\omega A_s(s) = 0 \qquad (9)$$

where E_s^{inc} is the tangential component of the incident electric field (or an impressed electric field as in the case of a driven antenna) and the potential functions represent the scattered field. Substituting (4) and (5) into (9) yields

$$\int_L ds' \frac{\partial}{\partial s'} I_s(s') \frac{\partial}{\partial s} G(s,s') + k^2 \int_L ds' I_s(s') \hat{s}\cdot\hat{s}' G(s,s') = -j\frac{4\pi k}{\eta} E_s^{\text{inc}}(s) \qquad (10)$$

an integrodifferential equation for the current distribution. Observing that (6) and (7) indicate

$$\frac{\partial}{\partial s} G(s,s') = -\frac{\partial}{\partial s'} G(s,s')$$

and integrating by parts (10) becomes

$$\int ds' \left[\frac{\partial^2}{\partial s'^2} + k^2(\hat{s}\cdot\hat{s}')\right] I_s(s') G(s,s') - \frac{d}{ds'} I_s(s') G(s,s') \Big|_0^L = -j\frac{4\pi k}{\eta} E_s^{\text{inc}}(s). \qquad (11)$$

If the wire of the loop is lossy, an internal impedance per unit length z^i may be defined

$$E_s^{\text{inc}}(s)_{\text{losses}} = -z^i I(s) \qquad (12)$$

which is added to the expression for the incident electric field component derived in Appendix A for the multiturn loop antenna driven symmetrically from both ends by magnetic ring sources. The radii of the magnetic rings are chosen to represent the actual source driving the loops (see Appendix A).

Inherent in the foregoing analysis are certain restrictions. For the thin-wire approximations to be valid, the radius of the wire helix must be much greater than the wire radius, and the wire radius must be much less than a wavelength. In this analysis the proximity effect on the circumferential current distribution is ignored; therefore, the inequality $p \geq 4a$ must be satisfied [9], [10].

Evidently the wire connecting the ends of the helix does not conform to the helical geometry. If the separation of the ends is small in terms of wavelength, a very simple procedure for obtaining the contribution of currents and charges on the wire connecting the ends may be used (see Appendix B).

NUMERICAL SOLUTION

A convenient numerical solution of the integrodifferential equation for the current distribution may be effected by the so-called method of moments [4]. A piecewise sinusoidal function is used to represent the current distribution as opposed to using the, perhaps more common, flat pulses or triangle pulses [7]. The current distribution is then

$$I_s(s') = \sum_{m=1}^{N} I_m(s') U(s';s_{m+1},s_m) \qquad (14)$$

where

$$I_m(s') = \frac{\alpha_{m+1}\sin k(s'-s_m) + \alpha_m \sin k(s_{m+1}-s')}{\sin k(s_{m+1}-s_m)} \qquad (15)$$

$$U(s';s_{m+1},s_m) = \begin{cases} 1, & s_m \leq s' < s_{m+1} \\ 0, & \text{otherwise} \end{cases}$$

and where $\{s_m\}$ is an ordered set of $N+1$ points along the axis of the wire including the end points. Furthermore, it is required that there be no discontinuity in the current at the wire ends.

Taking the derivative of the current distribution yields

$$\frac{d}{ds'} I_s(s') = \sum_{m=1}^{N} \left[\frac{d}{ds'} I_m(s')\right] U(s';s_{m+1},s_m). \qquad (16)$$

Operating on the current distribution with the Helmholtz operator yields

$$\left[\frac{d^2}{ds'^2} + k^2\right] I_s(s') = \sum_{m=1}^{N} \frac{d}{ds'} I_m(s')[\delta(s'-s_m) - \delta(s'-s_{m+1})] - \frac{d}{ds'} I_s(s')[\delta(s') - \delta(s'-L)]. \qquad (17)$$

By substituting (17) into (11) one obtains

$$\sum_{m=1}^{N} \left[\frac{d}{ds'} I_m(s') G(s,s') \Big|_{s'=s_m}^{s'=s_{m+1}} - k^2 \int_{s_m}^{s_{m+1}} ds' (1 - \hat{s}\cdot\hat{s}') I_m(s') G(s,s') - j\frac{4\pi k}{\eta} z^i I_m(s) U(s;s_{m+1},sm)\right] = -j\frac{4\pi k}{\eta} E_s^{\text{inc}}(s). \qquad (18)$$

A linear system of equations is obtained from (18) by the introduction of a convenient set of points on which (18) is satisfied. Also, the boundary conditions on the current must be enforced. For the multiturn loop the current boundary condition is

$$I_s(0) = I_s(L) \qquad (19)$$

or

$$\alpha_1 = \alpha_{N+1}. \tag{20}$$

Using (15) and (20) in (18) and satisfying (18) at points $s = s_n$, for $n = 1,2,\cdots,N$, one obtains

$$\sum_{m=1}^{N} \Pi_{nm}\alpha_m = \Gamma_n \tag{21}$$

where

$$\Pi_{n1} = [G(s_n,s_N) - [G(s_n,s_1) + G(s_n,s_{N+1})] \cdot \cos k\Delta_1 + G(s_n,s_2)] \frac{1}{k \sin k\Delta_1}$$
$$- \int_0^{s_2} ds' \, (1 - \hat{s}_n \cdot \hat{s}') \sin k(s_2 - s') G(s_n,s')/\sin k\Delta_1$$
$$+ \int_{s_N}^{L} ds' \, (1 - \hat{s}_n \cdot \hat{s}') \sin k(s' - L) G(s_n,s')/\sin k\Delta_1$$
$$- j \frac{4\pi z^i}{\eta k} \delta_{n1}. \tag{22}$$

For $m > 1$

$$\Pi_{nm} = \frac{G(s_n,s_{m-1}) - G(s_n,s_m) \cos k\Delta_{m-1}}{k \sin k\Delta_{m-1}}$$
$$+ \frac{G(s_n,s_{m+1}) - G(s_n,s_m) \cos k\Delta_m}{k \sin k\Delta_m}$$
$$+ \int_{s_{m-1}}^{s_m} ds' \, (1 - \hat{s}_n \cdot \hat{s}') \cdot \sin k(s_{m-1} - s') G(s_n,s')/\sin k\Delta_{m-1}$$
$$- \int_{s_m}^{s_{m+1}} ds' \, (1 - \hat{s}_n \cdot \hat{s}') \cdot \sin k(s_{m+1} - s') G(s_n,s')/\sin k\Delta_m - j \frac{4\pi z^i}{\eta k} \delta_{nm}. \tag{23}$$

For $n = 1,N$

$$\Gamma_n = -j \frac{4\pi E_s^{\text{inc}}(s_n)}{\eta k}. \tag{24}$$

Here $\Delta_m = s_{m+1} - s_m$, for all m. It may be noted that satisfying (18) at $s = s_{N+1} = L$ yields the same equation as satisfying it at $s = s_1 = 0$, provided that (20) is used.

APPLICATIONS

The characteristics of interest concerning the loop antenna are its impedance, efficiency, and pattern. Since the loop is driven from the wire ends with voltage V, the impedance is (see Appendix A and Fig. 1)

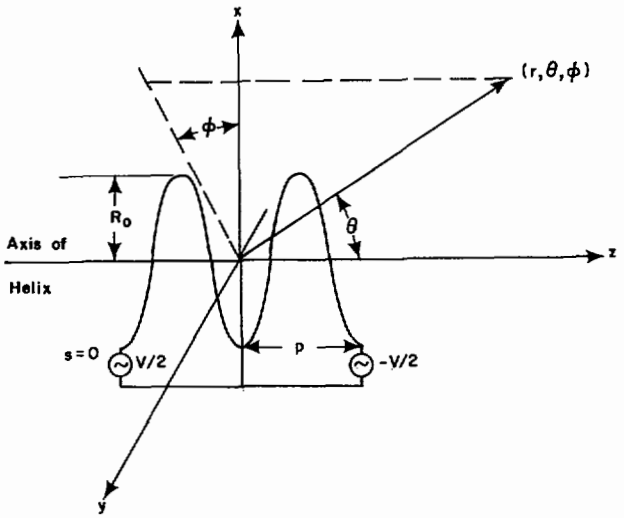

Fig. 1. Multiturn loop in form of circular helix shown with coordinate system.

$$Z_a = \frac{V}{I_s(0)} = \frac{V}{I_s(L)}. \tag{25}$$

The antenna efficiency is

$$\text{EFF (percent)} = \frac{[\text{Re}\,[Z_a]\,|\,I_s(0)\,|^2]_{z^i=0}}{[\text{Re}\,[Z_a]\,|\,I_s(0)\,|^2]_{z^i\neq 0}} \times 100. \tag{26}$$

For a solid or tubular conductor with a wall thickness that is large compared to the skin depth the internal impedance per unit length is [1]

$$z^i = (1 + j)(2\pi a\sigma\delta_s)^{-1}. \tag{27}$$

The skin depth δ_s is given by

$$\delta_s = (2/\omega\mu\sigma)^{1/2}. \tag{28}$$

To determine the field radiated from the loop, the restriction that the ends of the loop be separated a distance small compared to the wavelength is again imposed. Accordingly, the radiation pattern is essentially that of a single-turn loop with the current

$$I(\phi') = \sum_{n=1}^{NT} I_s[\{\phi' + 2(n-1)\pi\}/\alpha]. \tag{29}$$

Here NT is the number of turns and α is given in (3). Using (29) and standard techniques, the electric field components in the radiation zone are obtained in the following form:

$$E_\theta(r,\theta,\phi) = -j \frac{\eta V}{2\pi Z_a} \frac{\exp(-jkr)}{r} F_\theta(\theta,\phi)$$

$$E_\phi(r,\theta,\phi) = -j \frac{\eta V}{2\pi Z_a} \frac{\exp(-jkr)}{r} F_\phi(\theta,\phi)$$

where the pattern functions are

$$F_\theta(\theta,\phi) = \frac{kR_0 \cos\theta}{I_s(0)} \int_0^{2\pi} d\phi' \, I(\phi') \cdot \exp\left[jkR_0 \sin\theta \cos(\phi - \phi') \right] \sin(\phi - \phi')$$

$$F_\phi(\theta,\phi) = \frac{kR_0}{I_s(0)} \int_0^{2\pi} d\phi' \, I(\phi') \cdot \exp\left[jkR_0 \sin\theta \cos(\phi - \phi') \right] \cos(\phi - \phi').$$

The impedance of a multiturn loop antenna operating in the low frequency regime as given by King [14] is

$$Z_a = R_a + jX_a \tag{30}$$

where

$$R_a = \frac{\pi}{6} \eta (kR_0)^4 (NT)^2 + r_i \{ p + [(2\pi R_0^2) + p^2]^{1/2} \} NT \tag{31}$$

$$X_a = \eta k R_0 \left\{ NT \left[\ln \frac{8R_0}{a} - 2 \right] + 2 \sum_{i=1}^{NT} (NT - i) u(i) \right\} \tag{32}$$

$$u(i) = -\frac{2}{e_i} E(e_i) + \left(\frac{2}{e_i} - e_i \right) K(e_i)$$

$$e_i = [1 + p^2 i^2 / (2R_0)^2]^{-1}$$

with $K(e_i)$ and $E(e_i)$ as complete elliptic integrals of the first and second kinds, respectively, and r_i the internal resistance per unit length for the wire forming the loop antenna. The foregoing formula attributed to King has been simplified somewhat and extended to include losses. Further, it is modified in accordance with the geometric configuration considered here being different from that considered by King.

NUMERICAL RESULTS

First the impedances of 1-, 2- and 3-turn perfectly conducting loop antennas are shown in Table I. The impedances are compared with those from the low frequency approximation and the results from King and Harrison [6] for single turn loops. In general the agreement is quite favorable. At low frequency the real part of the integral equation solution is not as accurate as the low frequency approximation because of accumulative truncation errors in the numerical computations (the computer used to obtain the presented data is the UNIVAC 1106 that carries 8 significant figures in single precision computations). For example if the reactance is accurate to $\pm 0.1\ \Omega$ then the resistance is probably accurate only to within $\pm 0.1\ \Omega$. In any event the foregoing comparisons are sufficiently good to indicate the validity of the assumed driving mechanism and the computer program.

From the foregoing data it is seen that adding turns to the loop antenna not only lowers the resonant frequency but it also causes the resonances to become much sharper. This characteristic is also exhibited in Figs. 2 and 3,

TABLE I
MULTITURN LOOP IMPEDANCE

kR_0	Z_a		
	NT = 1	NT = 2	NT = 3
0.05	0.018 + j 60.0 (0.001 + j 61.1)* (0.0 + j 61.1)**	0.036 + j 166.3 (0.005 + j 193.6)*	0.057 + j298.9 (0.0111 + j 374.5*
0.10	0.087 + j 124 (0.020 + j 122)*	0.323 + j 477.1 (0.079 + j 387.2)*	8.75 + j3502
0.15	0.272 + j 197 (0.10 + j 183)* (0.13 + j 203)**	18.1 + j 3111	0.35 - j 627.6
0.20	0.762 + j 287 (0.316 + j 244)* (0.535 + j 296)**	2.58 - j 989.0	0.082 - j 273.8
0.25	2.38 + j 454 (1.82 + j 422)**	0.718 - j 432.6	0.026 - j 141.1
0.30	6.84 + j 656 (6.11 + j 614)**	0.386 - j 260.1	0.019 - j 53.0
0.35	23.1 + j 1018 (23.2 + j 967)**	0.241 - j 166.4	0.107 + j 29.0
0.40	118 + j 1929 (134 + j 1901)**	0.147 - j 101.1	0.637 + j 136.6
0.45	4023 + j 8492 (7942 + j 9076)**	0.085 - j 47.9	5.19 + j 388.1

$\Omega = 2\ \ell n(2\pi R_0/a) = 10.0$, $p = 0.0258$ m
$R_0 = 0.1524$ m, $z^i = 0$
*obtained from low frequency approximation
**obtained from King and Harrison [6]

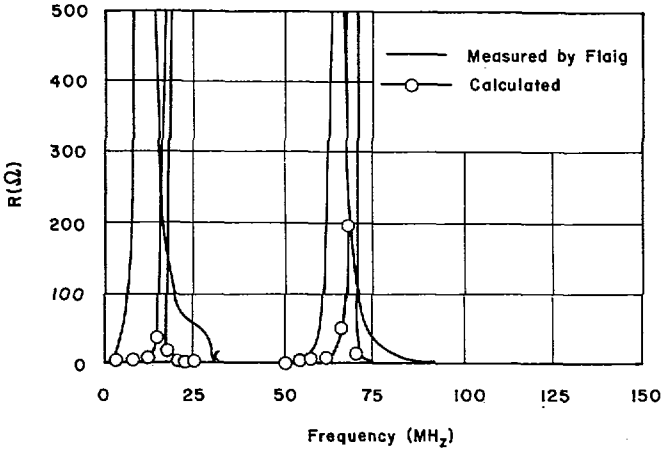

Fig. 2. Input resistance of a 5-turn copper wire loop antenna. $R_0 = 0.2$ m, $a = 0.00079$ m, and $p = 0.01$ m.

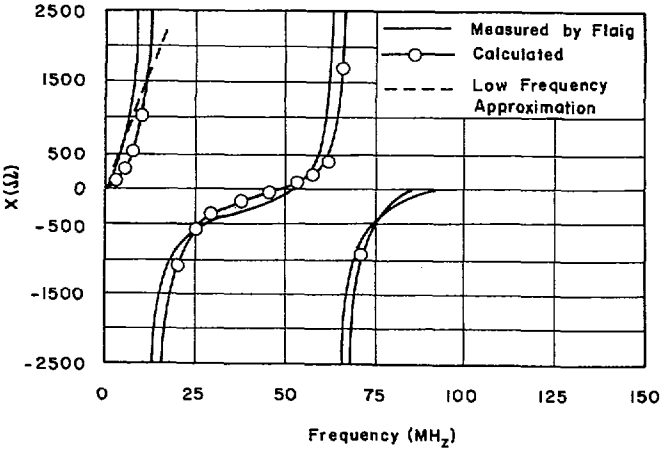

Fig. 3. Input reactance of 5-turn copper wire loop antenna. $R_0 = 0.2$ m, $p = 0.01$ m, and $a = 0.000794$ m.

where the antenna resistances and reactances are shown for a 5-turn copper wire loop antenna. The experimental results were obtained by Flaig [15]. For the calculated results the number of piecewise sinusoidal sections used is 82 while utilizing the symmetry of the antenna current distribution. The convergence of the numerical solution depended upon the wire radius as reported previously [18]. For that reason the computer program could not handle as thin a wire as Flaig used to construct his 5-turn loop antenna. The parameters of Flaig's antenna are $R_0 = 0.2$ m, $a = 0.000794$ m, and $p = 0.01$ m; the parameters used in the computer program are $R = 0.2$ m, $a = 0.005$ m, and $p = 0.02$ m. In both cases the same internal impedance per unit length of copper wire is used. The agreement between measured and calculated input reactances is quite good. However, the input resistances do not compare nearly as well; yet the agreement tends to improve at higher frequencies.

In making measurements Flaig considered his balum transformer (Anzac Model XT-617) behaved essentially as a transmission line (with phase velocity of free space) in series with a 4:1 impedance transformer. How these assumptions affected the antenna impedance measurements is not known. However, at low frequencies the experimentally determined transmission line characteristic impedance departed significantly from the assumed value based upon an average measured value for the frequency range from 50 to 150 MHz. The first resonance occurs well below 50 MHz. Furthermore, the low frequency approximation agrees better with the numerically obtained results. For example at $f = 12.5$ MHz the low frequency approximation yields $Z_a = 1.34 + j1539$; the integral equation solution is $Z_a = 1.52 + j1059$. Thus it is expected that experimental error accounts for a large part of the disagreement between the measured and calculated input resistances.

Antenna efficiency is an important consideration for the multiturn loop. Flaig used an analysis developed by Munk [16] to compute the efficiency as well as the radiation resistance (Munk did not obtain the reactance). Theoretical and experimental results are shown in Fig. 4 for a 5-turn copper wire loop. At low frequencies, even past the first resonance, the antenna efficiency of the 5-turn loop is poor. But near the second resonance the efficiency tends to improve.

Field patterns of the 1-, 2-, and 3-turn loop antennas are shown in Figs. 5 and 6. The patterns are for conditions near the first resonance of the antennas. Apparently the patterns of multiturn loops below the first resonance are similar to the low frequency pattern of a single turn loop.

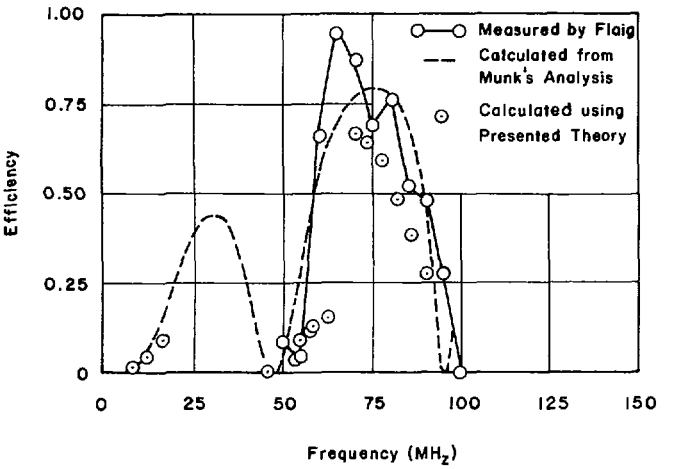

Fig. 4. Antenna efficiency of 5-turn copper wire loop. $R_0 = 0.2$ m, $a = 0.000794$ m, and $p = 0.01$ m.

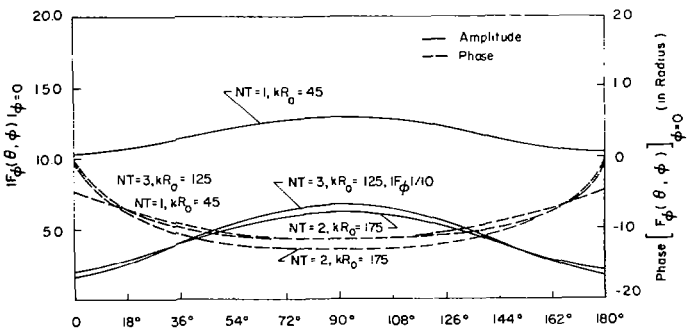

Fig. 5. Field patterns of 1-turn, 2-turn, and 3-turn loop antennas. $\Omega = 2 \ln (2\pi R_0/a) = 10.0$, $p = 4a$, and $N = 50$. (For these data $|F_\theta| \ll |F_\phi|$.)

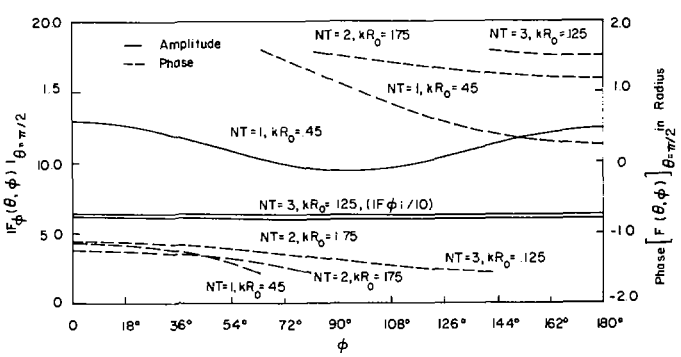

Fig. 6. Field patterns of 1-turn, 2-turn, and 3-turn loop antennas. $\Omega = 2 \ln (2\pi R_0/a) = 10.0$, $p = 4a$, and $N = 50$. (For these data $|F_\theta| \ll |F_\phi|$.)

APPENDIX A

For convenience the loop antennas are considered to be driven from magnetic current sources. These magnetic sources may represent the equivalent field distribution in the driving gap region such as the open end of a transmission line [17]. Recently Tsai [12] has derived expressions for the field about two magnetic current sources: the magnetic frill and the magnetic current ring. The magnetic frill is the magnetic current equivalent to the TEM mode field distribution in the gap of an open-ended coaxial transmission line connected to a perfectly conducting plane and the magnetic ring is the magnetic current equivalent to the field distribution in an infinitesimally thin circumferential slot driving a cylindrical antenna.

One of the advantages of using the aforementioned magnetic current sources is that analytic expressions are

available for the field about the sources. For example the field along the axis of a magnetic ring is

$$E_z(\rho,z,\phi)\,|_{\rho=0} = -\frac{Va}{2}\frac{\partial}{\partial a}K(z,z_0) \qquad \text{(A1)}$$

where a is the radius of the ring and

$$K(z,z_0) = \frac{\exp\left[-jk((z-z_0)^2+a^2)^{1/2}\right]}{((z-z_0)^2+a^2)^{1/2}}$$

with z_0 locating the center of the ring along the z axis and V the voltage impressed across the equivalent infinitesimal gap. It is straightforward to extend (A1) to represent the axial electric field produced by the equivalent magnetic currents for a general gap excitated antenna. The result is

$$E_z(\rho,z,\phi)\,|_{\rho=0} = +\frac{a}{2}\int_{\text{gap}}\left[\frac{\partial}{\partial a}K(z,z')\right]E_z^{\text{gap}}(z')\,dz'. \qquad \text{(A2)}$$

However, the foregoing result requires a determination of the electric field impressed in the gap. Unfortunately this electric field is not generally known *a priori*.

When (A1) or (A2) is used for the impressed field the integral equation for the current distribution is obtained by requiring the total z-component of the electric field to be zero along the wire axis. This procedure is the application of the so called extended boundary condition as discussed by Taylor and Wilton [18]. The use of (A1) and the extended boundary condition should be mathematically equivalent to the use of the delta gap feed and the boundary condition on the tangential component of the electric field at the antenna surface. The latter procedure encounters difficulties when a colocation solution technique is used such as is presented in the foregoing.

At large distances from the gap, i.e., $z \gg$ gap width, (A2) yields that the electric field produced by the equivalent sources for a finite gap is essentially the same as that produced by an infinitesimally thin magnetic current ring. However, at points near the gap where $k((z-z_0)^2+a^2)^{1/2} < 0.1$

$$E_z(\rho,z,\phi)\,|_{\rho=0} \simeq -\frac{a^2}{2}\int_{\text{gap}}\left[\frac{1}{R^3}+\frac{k^2}{2R}\right]E_z^{\text{gap}}(z')\,dz' + j\frac{k^3a^2}{6}\int_{\text{gap}}E_z^{\text{gap}}(z')\,dz' \qquad \text{(A3)}$$

where $R = ((z-z')^2+a^2)^{1/2}$. A convenient approximation for the electric field in the gap is[1]

$$E_z^{\text{gap}}(z) \simeq -\frac{V_0}{w_g}$$

where w_g is the gap width, so that (A3) becomes for $z_0 = 0$, $z = 0$

$$E_z(\rho,z,\phi)\,|_{\rho=0;\,z=0} \simeq \frac{V}{2}\frac{1}{(a^2+(w_g/2)^2)^{1/2}}. \qquad \text{(A4)}$$

[1] This approximation is well known to yield good antenna impedances [19].

For a infinitesimally thin magnetic current ring with radius a_s the axial component of the electric field at the center of the ring is $V/2a_s$. Thus (A4) may be used to define an equivalent radius of a infinitesimally thin ring to represent a band of magnetic current. This equivalent radius is

$$a_s = (a^2+(w_g/2)^2)^{1/2}.$$

The multiturn loop is then considered to be driven from both ends by equivalent magnetic current rings. This is a reasonable alternative to driving the loop from the center of the wire connecting the ends of the windings since the separation of the ends of the windings is an electrically short distance. Unfortunately when considering the loop antenna, knowing the field along the axis of the magnetic ring is not sufficient. In this case the electric field component tangent to the loop axis must be known. There are two available routes to be taken. First, one may numerically compute this field component as Tsai did, or one may judiciously obtain an approximation that is convenient for computations. The latter approach will be followed.

At distances that are large in comparison with the radius of the magnetic ring, the field distribution is essentially that of an electric dipole with moment

$$\boldsymbol{P} = \pi a_s^2 \epsilon V \hat{z}.$$

The electric field about a dipole is

$$\boldsymbol{E}(r) = \frac{\exp(-jkr)}{4\pi\epsilon}\left[\left(\frac{1}{r^3}+j\frac{k}{r^2}\right)[3\hat{r}(\hat{r}\cdot\boldsymbol{P})-\boldsymbol{P}] - \frac{k^2}{r}[\hat{r}\times(\hat{r}\times\boldsymbol{P})]\right] \qquad \text{(A5)}$$

where r is the radius vector from the dipole to the point of observation. (It is readily noted that (A5) has the same far field behavior as obtained by Tsai, provided $ka \ll 1$.) Furthermore, it is observed that (A5) reduces to (A1) along the z axis when $r \to R_s = (r^2+a_s^2)^{1/2}$. Even with $r \to R_s$, (A5) still exhibits the proper far-field behavior. Therefore, the component of the illuminating electric-field tangent to the wire loop at point s is approximately

$$E_s^{\text{inc}}(s) = \frac{\exp(-jkR_s)}{4}Va_s^2\left[\left(\frac{1}{R_s^3}+j\frac{k}{R_s^2}\right)\cdot[3(\hat{r}\cdot\hat{s})(\hat{r}\cdot\hat{z})-\hat{s}\cdot\hat{z}] - \frac{k^2}{R_s}\hat{s}\cdot[\hat{r}\times(\hat{r}\times\hat{z})]\right] \qquad \text{(A6)}$$

where $\hat{s}$ is the unit vector tangent to the axis of the wire forming the loop and $R_s = (R^2(s,s_0)+a_s^2)^{1/2}$ with R given by (7). Note that (A6) is precise very near the magnetic ring $R(s,s_0) \sim a$ and at distances $R(s,s_0) \gg a^2$.

For a single turn circular loop driven from a magnetic ring source at $s_0 = 0$, the incident field component driving

the wire loop is

$$E_s^{\text{inc}}(s) = \frac{a_s^2 V}{2}\left[\frac{1}{2R_s^2}\left[jk + \frac{1}{R_s}\right]\left[1 + \cos^2\frac{\alpha s}{2}\right] - \frac{k^2}{2R_s}\sin^2\frac{\alpha s}{2}\right]\exp(-jkR_s) \quad \text{(A7)}$$

where

$$R_s = ((2R_0 \sin \alpha s/2)^2 + a_s^2)^{1/2}.$$

Using (A7), results are obtained that agree to within a few percent with those presented by King and Harrison [6].

APPENDIX B

In this appendix a procedure is developed to account for the wire segment connecting the ends of the helical loop. The contribution to the incident field from the current and charge sources on the subject wire segment may be expressed.

$$E_s^{\text{cor}}(s) = -j\frac{\eta}{4\pi k}\int_0^{\Delta L} dz' \frac{\partial}{\partial z'} I_z(z') \frac{\partial}{\partial s} G_1(s,z') + k^2(\hat{s}\cdot\hat{z}) I_z(z') G_1(s,z') \quad \text{(B1)}$$

where the wire segment is parallel to the z axis and extends from $z' = 0$ to $z' = \Delta L = pNT$. The number of loop turns is designated by NT. Also,

$$\hat{s}\cdot\hat{z} = \frac{\alpha p}{2\pi} = \frac{\Delta L}{L} \quad \text{(B2)}$$

and

$$G_1(s,z) = \frac{\exp[-jk((2R_0 \sin \alpha s/2)^2 + (\alpha p s/2\pi - z')^2 + a^2)^{1/2}]}{((2R_0 \sin \alpha s/2)^2 + (\alpha p s/2\pi - z')^2 + a^2)^{1/2}}. \quad \text{(B3)}$$

After some mathematical manipulation (B1) becomes

$$E_s^{\text{cor}}(s) = j\frac{\eta}{4\pi k}\left[\frac{\Delta L}{L}\frac{\partial}{\partial z'} I_z(z') G_1(s,z')\Big|_{z'=0}^{z'=\Delta L} - \frac{\Delta L}{L}\int_0^{\Delta L} dz' \left[\left(\frac{d^2}{dz'^2} + k^2\right) I_z(z')\right] G_1(s,z') - \alpha R_0^2 \sin \alpha s \int_0^{\Delta L} dz' \frac{\partial}{\partial z'} I_z(z') \frac{1}{R}\frac{\partial}{\partial R}\cdot\left[\frac{\exp(-jkR)}{R}\right]\right] \quad \text{(B4)}$$

where

$$R^2 = [2R_0 \sin(\alpha s/2)]^2 + (\alpha p s/2\pi - z')^2 + a^2. \quad \text{(B5)}$$

Over the short-wire segment the current distribution may be considered sinusoidal; i.e.,

$$I_z(z) = \frac{I_z(0)\sin k(\Delta L - z) + I_z(\Delta L)\sin kz}{\sin k\Delta L}. \quad \text{(B6)}$$

From the symmetry of the excitation

$$I_z(0) = I_z(\Delta L) = I_s(0)$$

then

$$I_z(z) = I_s(0)\frac{\sin k(\Delta L - z) + \sin kz}{\sin k\Delta L}. \quad \text{(B7)}$$

Substituting (B7) into (B4) results in the vanishing of the first integral of (B4). The resulting form for E_s^{cor} is then added to the incident field in the integral equation for the antenna current distribution. Without this correction, meaningless results are generally obtained for the antenna current distribution.

ACKNOWLEDGMENT

The authors thank V. Richard of the Ballistics Research Laboratories for suggesting the problem.

REFERENCES

[1] R. W. P. King, "The loop antenna for transmission and reception," in *Antenna Theory*, Part 1, R. E. Collins and F. J. Zucker, Eds. New York: McGraw-Hill, 1969, pp. 458–482.
[2] B. R. Rao, "Far field patterns of large circular loop antennas: Theoretical and experimental results," *IEEE Trans. Antennas Propagat.* (Commun.), vol. AP-16, pp. 269–270, Mar. 1968.
[3] A. Baghdasarian and D. J. Angelakos, "Scattering from conducting loops and solution of circular loop antennas by numerical methods," *Proc. IEEE*, vol. 53, pp. 818–822, Aug. 1965.
[4] R. F. Harrington and J. L. Ryerson, "Electromagnetic scattering by loaded wire loops," *Radio Sci.*, vol. 1, pp. 347–352, Mar. 1966; also correction, vol. 1, Dec. 1966.
[5] J. L. Lin and K. M. Chen, "Resonances of loops," *IEEE Trans. Antennas Propagat.* (Commun.), vol. AP-15, pp. 477–478, May 1967.
[6] R. W. P. King and C. W. Harrison, Jr., *Antennas and Waves: A Modern Approach*. Cambridge, Mass.: M.I.T. Press, 1969, ch. 9.
[7] G. A. Richards, "Computer analysis of polygon loop antennas," Electro-Science Lab., Ohio State Univ., Tech. Rep. 2708-5, Dec. 17, 1969.
[8] G. A. Richards, "Computer analysis of three-dimensional loop antennas," Electro-Science Lab., Ohio State Univ., Rep. 2708-6, 1970.
[9] T. Padhi, "Theory of coil antennas," *Radio Sci. J. Res. Nat. Bur. Stand.*, vol. 69D, pp. 997–1001, July 1965.
[10] G. Smith, "The radiation efficiency of electrically small multiturn loop antennas," *IEEE Trans. Antennas Propagat.* (Commun.), vol. AP-20, pp. 656–657, Sept. 1972.
[11] C. D. Taylor, "Electromagnetic scattering from arbitrary configurations of wires," *IEEE Trans. Antennas Propagat.* (Commun.), vol. AP-17, pp. 662–663, Sept. 1969.
[12] L. L. Tsai, "A numerical solution for the near and far fields of an annular ring of magnetic current," *IEEE Trans. Antennas Propagat.*, vol. AP-20, pp. 569–576, Sept. 1972.
[13] R. E. Collin and F. J. Zucker, Eds., *Antenna Theory*, Part I. New York: McGraw-Hill, 1969, ch. 2.
[14] R. W. P. King, *Fundamental Electromagnetic Theory*. New York: Dover, 1963, ch. 6, sect. 15.
[15] T. L. Flaig, "The impedance and efficiency of multi-turn loop antennas," Electro-Science Lab., Ohio State Univ., Rep. 2235-3, 1968.
[16] B. A. Munk and T. L. Flaig, "Radiation resistance and efficiency of multiturn loop antennas," Electro-Science Lab., Ohio State Univ., Rep. 2235-4, 1968.
[17] E. C. Jordan and K. G. Balmain, *Electromagnetic Waves and Radiating Systems* (second edition). Englewood Cliffs, N. J.: Prentice-Hall, 1968, ch. 13, sect. 5.
[18] C. D. Taylor and D. R. Wilton, "The extended boundary condition solution of the dipole antenna of revolution," *IEEE Trans. Antennas Propagat.* (Commun.), vol. AP-20, pp. 772–776, Nov. 1972.
[19] R. F. Harrington, *Field Computation by Moment Methods*. New York: Macmillan, 1968, ch. 4.